Helically Annelated and Cross-Conjugated β-Oligothiophenes: A Fourier Transform Raman Spectroscopic and Quantum Chemical Density Functional Theory Study

Reyes Malavé Osuna,[†] Rocío Ponce Ortiz,[†] Víctor Hernández,[†] Juan Teodomiro López Navarrete,*[,†] Makoto Miyasaka,[‡] Suchada Rajca,[‡] Andrzej Rajca,[‡] and Rainer Glaser[§]

Department of Physical Chemistry, University of Málaga, 29071-Málaga, Spain, Department of Chemistry, University of Nebraska, Lincoln, Nebraska 68588-0304, and Department of Chemistry, University of Missouri−Columbia, Columbia, Missouri 65211

Received: November 21, 2006

Ⓦ **This paper contains enhanced objects available on the Internet at http://pubs.acs.org/jpcc.**

This article describes Fourier transform Raman/infrared spectroscopic studies to determine the conjugational properties of novel β-oligothiophenes, in which thiophene rings are helically annelated, forming a cross-conjugated π-system. These helicenes may be viewed as fragments of the unprecedented carbon−sulfur $(C2S)_n$ helix, having a sulfur-rich molecular periphery. The B3LYP/6-31G** vibrational analysis of the experimental spectroscopic data for β-oligothiophenes with three, seven, and eleven thiophene rings indicates selective enhancement of a limited number of Raman scatterings. In particular, the enhancement of the Raman-active skeletal ν(C═C) stretching modes in the 1400−1300-cm^{-1} region is related to the occurrence of a vibronic coupling between the highest-occupied molecular orbital and lowest-unoccupied molecular orbital frontier molecular orbitals. Decreased dispersion of enhanced Raman scatterings and greatly increased near degeneracy of the highest occupied MOs with the increasing number of annelated thiophene rings suggest significant electron localization in β-oligothiophenes, similar to that in cross-conjugated π-systems.

I. Introduction

Oligothiophenes are among the most studied π-systems for organic materials, including applications as active components in electronic or optical devices.[1] The research in this area has been focused on α-oligothiophenes, such as α-sexithiophene, in which thiophene rings are connected with single CC bonds at α-positions, forming a linearly extended, conjugated π-system (Figure 1).[2−11] Annelated α-oligothiophenes, such as trithienoacenes, pentathienoacene, and heptathienoacene, have been prepared.[12−15] Recent studies of the materials derived from these linearly annelated π-systems with relatively rigid structures suggested significantly improved optical and electronic properties.[16,17] However, the synthesis and studies of analogous β-oligothiophenes, in which thiophene rings are connected with single CC bonds at β-positions, remain relatively unexplored,[18−22] in part due to the lack of efficient synthetic methodologies, and due to the fact that the β−β linkages thiophenes are susceptible to twisting, leading to interruption of π−π overlap. Recent developments of synthetic methodologies for thiophene-based annelation of β-oligothiophenes provide a novel class of β-oligothiophenes, in which *n* thiophene rings are helically annelated, forming [*n*]helicene, such as[7]helicene (Figure 1).[23−27]

As fragments of the carbon−sulfur $(C_2S)_n$ helix, annelated β-oligothiophenes possess a cross-conjugated carbon−carbon framework, with all sulfur atoms positioned at the molecular periphery. The presence of multiple short intermolecular S···S contacts, as well as π-stacking of the curved π-systems, is promising for exploration of transport properties.[25,28−30] In recent work on achiral cross-conjugated π-systems, unusually robust optical properties were reported; however, studies of their electronic properties are in the early stages.[31−37]

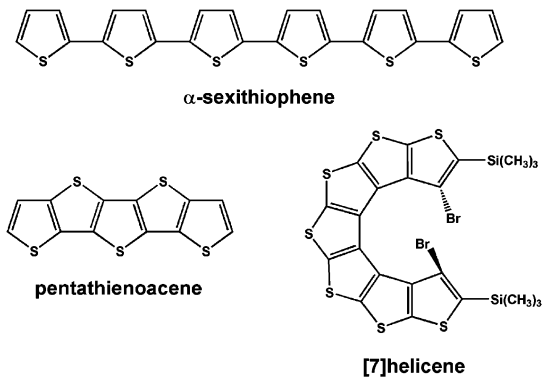

Figure 1. Oligothiophenes: α-oligothiophene (α-sexithiophene), annelated α-oligothiophene (pentathienoacene), and annelated β-oligothiophene ([7]helicene).

A series of alkyl-substituted annelated β-oligothiophenes with up to 11 thiophene rings have been prepared (Figure 2). It has been shown that such structures possess moderate helical curvatures, thus still allowing for significant π−π overlap within the cross-conjugated π-system for the carbon−carbon framework.[26] Therefore, such β-oligothiophenes provide a unique opportunity for systematic study of helical cross-conjugated π-systems.

Vibrational spectroscopy is an excellent tool to determine relationships between structure and properties, to guide the design of new molecular materials with an improved behavior.

* To whom correspondence should be addressed. E-mail: Teodomiro@uma.es.
[†] University of Málaga.
[‡] University of Nebraska.
[§] University of Missouri−Columbia.

10.1021/jp0677344 CCC: $37.00
Published on Web 01/18/2007

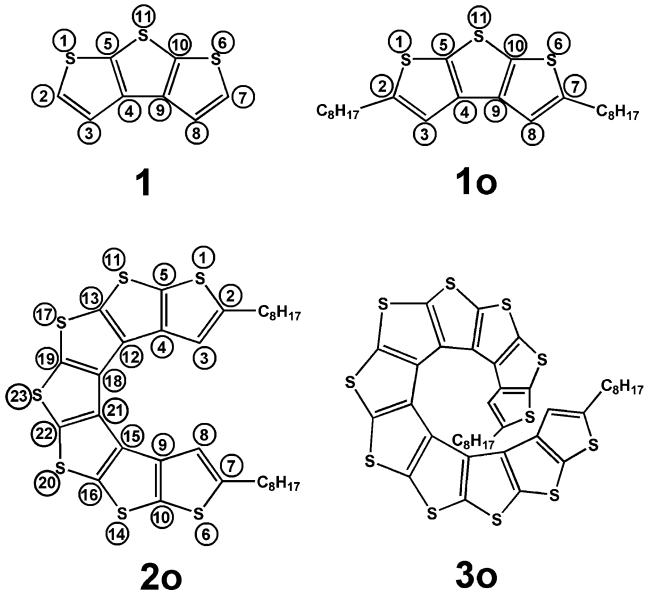

Figure 2. Octyl-substituted helically annelated β-oligothiophenes studied in this work.

In particular, Raman spectroscopy is well suited for the analysis of all classes of π-conjugated systems. Raman frequencies and intensities have been routinely correlated with optical and electronic signatures of oligothiophenes with structures that contain a π-conjugated backbone.

The effective conjugation coordinate (ECC) model,[38] developed by Zerbi and co-workers, has been widely applied to predict two main trends of variation for the Raman spectral fingerprints of π-conjugated molecules: (a) Selective enhancement of a few Raman scatterings associated with collective C=C/C−C stretching vibrations of the π-conjugated framework. Such selective phenomenon in these types of one-dimensional π-systems of linear chain largely involves an electron−phonon coupling, which is the origin of their outstanding optical and electrical features. (b) Frequency downshift of the enhanced Raman lines upon structural relaxation of the system, as the consequence of either a greater π-electron conjugation/delocalization in the neutral state or partial quinoidization of the π-conjugated framework induced by chemical doping. The ECC model relies on the analysis of the experimental spectroscopic data and the vibrational eigenvectors obtained from reliable quantum chemical calculations, providing precisely relevant molecular parameters that would be very difficult to evaluate by other conventional experimental techniques. The first-principles quantum chemical calculations within density functional theory (DFT) theory are well suited to model extended π-conjugated systems because DFT theory accounts for electron correlation effects.

Raman spectra of various π-conjugated systems have been reported, including those of molecules with rather complex molecular architectures and substitution patterns.[39] The ECC model has been successfully applied in the studies of a series of π-conjugated oligoheterocycles (i.e., with the adjacent α-linked units arranged in a linear or cyclic fashion), as well as in acenes and heterocenes with a nearly flat π-conjugated framework. However, experimental studies of molecules with helical structures ([*n*]helicenes) by Raman spectroscopy are absent to our knowledge,[40,41] in spite of the increasing interest in [*n*]helicenes,[42] especially as building blocks for chiral materials.[43] Although rare examples of Raman spectra for the cross-conjugated π-systems have appeared, rigorous vibrational analyses, using the first-principle quantum chemical computations within the ECC model, were not reported.[37,44,45]

In this article, we report the spectroscopic Raman scattering of helically annelated β-oligothiophenes with significant π−π overlap within the cross-conjugated π-system for the carbon−carbon framework. The experimental Raman spectra are analyzed with the aid of B3LYP/6-31G** vibrational computations. Our analyses, based upon the ECC model, indicate that the selective enhancements of the Raman scatterings in the 1400−1300-cm^{-1} spectral region are related to totally symmetric ν(C=C) stretching modes, which strongly couple to the highest-occupied molecular orbital (HOMO) and lowest-unoccupied molecular orbital (LUMO) frontier orbitals.

II. Experimental and Theoretical Methods

Synthesis and purification of the helically annelated and cross-conjugated oligothiophenes were described elsewhere.[26,27] Fourier transform infrared (FTIR) absorption spectra were recorded on a Bruker Equinox 55 spectrometer. Compounds were ground to a powder and pressed in KBr pellets. FTIR spectra, with a standard spectral resolution of 2 cm^{-1}, were collected as the average of 50 scans. Interference from atmospheric water vapor was minimized by purging the instrument with dry argon before starting the data collection. FT Raman scattering spectra were collected on a Bruker FRA106/S apparatus and a Nd:YAG laser source (λ_{exc} = 1064 nm), in a back-scattering configuration. The operating power for the exciting laser radiation was kept to 100 mW in all the experiments. Samples were analyzed as pure solids in sealed capillaries. Typically, 1000 scans with 2-cm^{-1} spectral resolution were averaged to optimize the signal-to-noise ratio.

DFT calculations were carried out using the Gaussian 03 program[46] running on SGI Origin 2000 and Altrix supercomputers. Becke's three-parameter exchange functional combined with the LYP correlation functional (B3LYP)[47] was employed, because it has been shown that the B3LYP functional yields similar geometries for medium-sized molecules as those obtained from the MP2 calculations with the same basis sets.[48,49] Moreover, the DFT force fields calculated using the B3LYP functional yield infrared spectra in very good agreement with experiments.[50,51] In particular, both geometries and vibrational circular dichroism (VCD) spectra, calculated at the B3LYP/6-31G* level of theory, showed excellent agreement with the experimental data (single-crystal X-ray structure and VCD spectra in chloroform) for a carbon-sulfur[7]helicene (Figure 1).[40] The standard 6-31G** basis set was used to obtain optimized geometries on isolated entities.[52] For the resulting ground-state optimized geometries, harmonic vibrational frequencies, and infrared and Raman intensities were calculated with the B3LYP functional. In the calculations, octyl side chains were replaced by methyl groups to reduce the computing cost; dioctyl- and dimethyl-substituted β-oligothiophenes are denoted with o and m, respectively, e.g., **1o** for 5,5′-dioctyldithieno-[2,3-*b*:3′,2′-*d*] thiophene.

Calculated harmonic vibrational frequencies were uniformly scaled down by a factor of 0.96 for the 6-31G** calculations, as recommended by Scott and Radom.[50] This scaling procedure typically has an adequate accuracy for a reliable assignment of the experimental data. Thus, all vibrational frequencies reported in this work are scaled values. The theoretical spectra were obtaining by convoluting the scaled frequencies with Gaussian functions (10 cm^{-1} width at the half-height). The relative heights of the Gaussians were determined from the theoretical Raman scattering activities. Molecular orbital contours and animations of vibrations were generated using Molekel 4.3.[53]

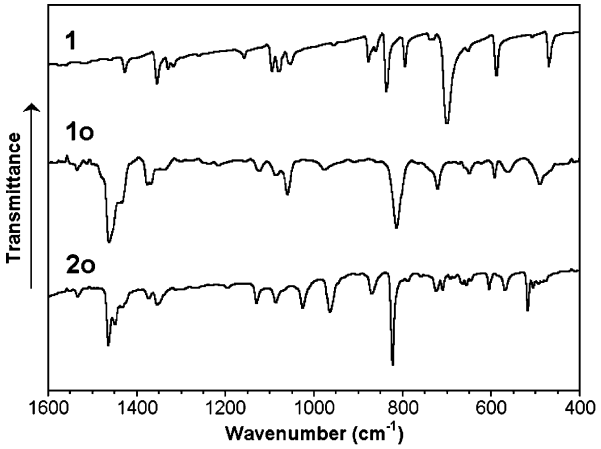

Figure 3. FT IR spectra of **1**, **1o**, and **2o** in the 1600−400-cm^{-1} wavenumber range.

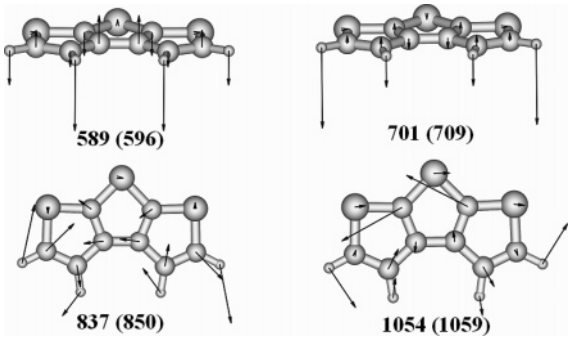

Figure 4. B3LYP/6-31G** vibrational eigenvectors related to some of the strongest IR bands of **1**. Experimental wavenumbers are given in cm^{-1}. Calculated wavenumbers, after scaling by a factor of 0.96, are shown in parenthesis.

III. Results and Discussion

IR Spectroscopy. Solid-state FTIR spectral profiles for **1**, **1o**, and **2o** are complex, with the most intense absorption bands found in the low-frequency range below 900 cm^{-1} (Figure 3). Correlations of their IR active bands with the computed B3LYP/6-31G** vibrational eigenvectors reveal that most of the low-frequency IR features originate from different out-of-plane γ(C−H) and in-plane δ_{ring} bending modes and hence that they are fully decoupled from the π-electron degree of freedom (Figure 4).

Raman Spectroscopy. The solid-state Raman spectra of the annelated β-oligothiophenes show characteristic profiles, with increasing number of selective and strong enhancement of the Raman scatterings in the 1500−1300-cm^{-1} region, as the number of annelated thiophene rings increases (Figures 5 and 6). The relative intensities of these scatterings steadily increase on going toward lower frequencies. Notably, these enhanced Raman scatterings appear less disperse (and shifted to lower frequency), with the increasing number of the annelated thiophene rings. The experimental peak positions are in excellent agreement with the computed B3LYP/6-31G** Raman spectra (Figure 7). Vibrational eigenvectors related to the strongest Raman scatterings of **1**, **2o**, and **3o** (Figure 8) are consistent with the assumption that these selectively enhanced Raman lines arise from similar skeletal ν(C═C) stretching modes. Therefore, it is probable that cross-conjugated C═C bonds become softened with the increasing number of annelated thiophene rings; such softening may also be varying within each β-oligothiophene, reaching its maximum for the C═C bonds of the middle thiophene rings. These experimental observations and computationally based interpretations for these helically annelated β-oligothiophenes should be compared to those reported for typical π-conjugated systems, including α-oligothiophenes, as predicted by the ECC model.

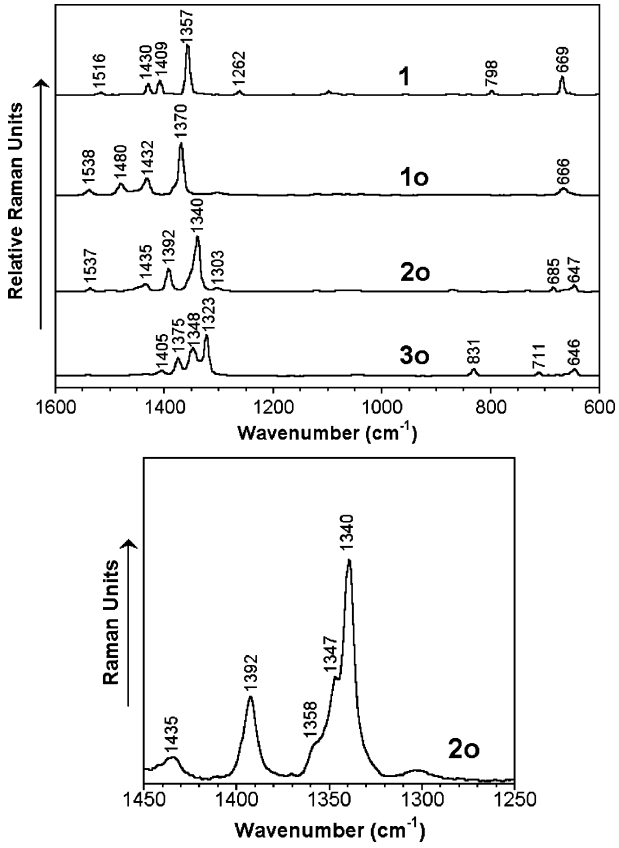

Figure 5. Solid-state FT Raman spectra of the annelated β-oligothiophenes (top) and high-resolution spectrum of **2o**. The Nd:YAG laser excitation (λ_{exc}) wavelength was 1064 nm.

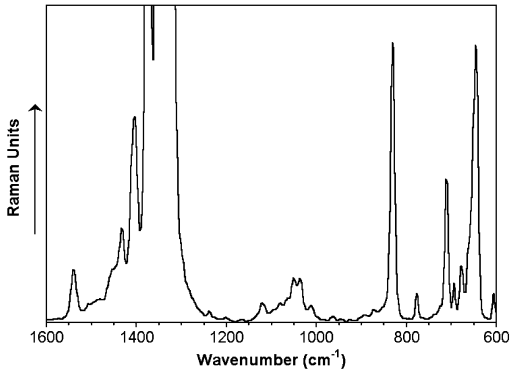

Figure 6. Enlarged profile of the solid-state Raman spectral profile of **3o**, showing the selective enhancement of particular Raman scatterings above 1300 cm^{-1}.

In aromatic or heteroaromatic polyconjugated chains, the ECC vibrational coordinate has the analytic form of a linear combination of ring C═C/C−C stretching modes, which belongs to the totally symmetric species and points toward the direction of a structural evolution of the π-conjugated system from a benzenoid-like pattern (usually that of the ground electronic state) to a quinoid-like one (that corresponding to the electronically excited state). The ECC model states that the totally symmetric skeletal C═C/C−C stretching vibrations mostly involved in the lattice dynamics of this collective ECC coordinate (i.e., those which give rise to the few and selectively enhanced Raman lines) should experience significant dispersions, both in peak

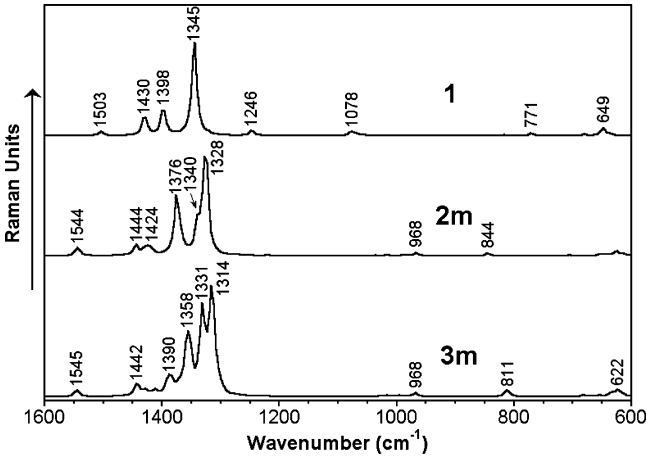

Figure 7. Theoretical B3LYP/6-31G** Raman profiles for **1, 2m**, and **3m.**

positions and intensities, upon increasing size of the π-conjugated backbone within a given series of neutral oligomers. In this regard, the experimental detection of changes in Raman frequencies and intensities with variable chain length constitutes a very useful way to evaluate the effectiveness of the π-conjugation for a particular family of α-linked oligoheteroaromatics. In addition, upon chemical or electrochemical doping of these π-conjugated α-oligoheterocycles, various types of quinoid-like charged species are created.[54] In this regard, the increasing degree of quinoidization of the π-conjugated backbone upon the progressive injection or removal of a first, second, or third electron, and so on, also gives rise to a steady red shift of the overwhelmingly strong Raman scatterings (i.e., due to the continuous softening of the conjugated framework of C═C bonds). This spectroscopic Raman information is quite valuable in elucidation of the charged carriers resulting from the various redox processes (e.g., radical cations or anions, dications, and dianions).[55−58]

The B3LYP/6-31G** electronic contours for MOs of **1** are shown in Figure 9. It is apparent that the most intense ν(C═C) stretching mode of **1** at 1357 cm^{-1} is strongly coupled to both the HOMO and LUMO frontier molecular orbitals. This result may be rationalized in terms of the bonding/antibonding interactions between the two innermost pairs of C_α and C_β atoms. When **1** is distorted along the 1357-cm^{-1} Raman-active vibrational mode, in the direction shown in Figure 8, the antibonding and bonding interactions in the LUMO and HOMO become weaker, respectively. Consequently, the LUMO becomes significantly stabilized and the HOMO becomes destabilized in energy along such molecular vibration. On the other hand, when **1** becomes distorted along the in-plane δ_{ring} bending mode of 669 cm^{-1} (Figures 8 and 9), the antibonding interactions in the LUMO between each S atom and its two nearest C_α atoms become weaker, while the corresponding bonding interactions in the HOMO between the S and C_α atoms at both ends of **1** also experience a weakening. Hence, the Raman-active in-plane δ_{ring} vibration of 669 cm^{-1} lowers the LUMO's energy while it raises the HOMO's energy. Upon structural distortion of **1** along the stretching mode of 1430 cm^{-1} the LUMO is stabilized because the antibonding C(2)−C(3) and C(7)−C(8) interactions in the LUMO become weaker, while the bonding C(4)−C(9) interaction are enhanced. However, the HOMO is destabilized to a much lower extent by this Raman mode, since the antibonding C(4)−C(9) interaction is the only one unfavorably forced by a distortion of **1** similar to that shown in Figure 8 for the B3LYP/6-31G** vibrational eigenvector of 1430 cm^{-1}. Finally, along the Raman-active mode of 1409 cm^{-1}, the antibonding C(2)−C(3) and C(4)−C(5) interactions in the LUMO within one-half molecule become weaker, while their symmetry-equivalent antibonding C(7)−C(8) and C(9)−C(10)

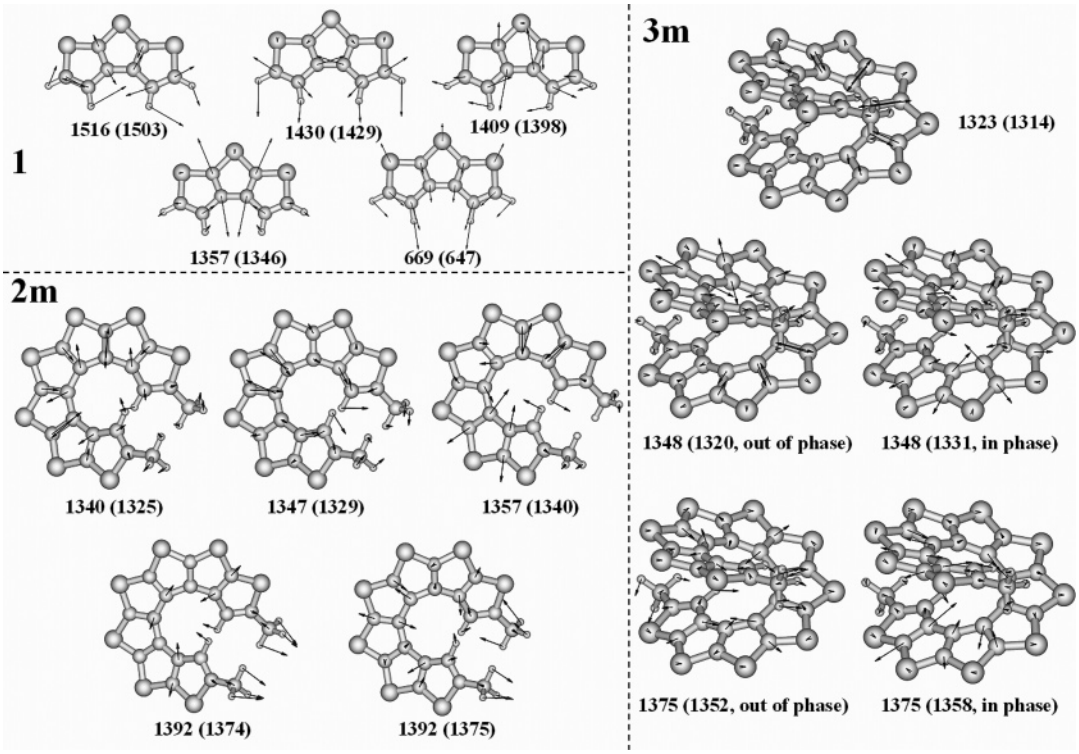

Figure 8. B3LYP/6-31G** vibrational eigenvectors associated with the most outstanding Raman features. Experimental wavenumbers are given in cm^{-1}. Calculated wavenumbers, after scaling by a factor of 0.96, are shown in parentheses.

Ⓦ The online version of this paper contains web-enhanced objects that show animations of the vibrational modes of Ⓦ **1m**, Ⓦ **2m**, and Ⓦ **3m**.

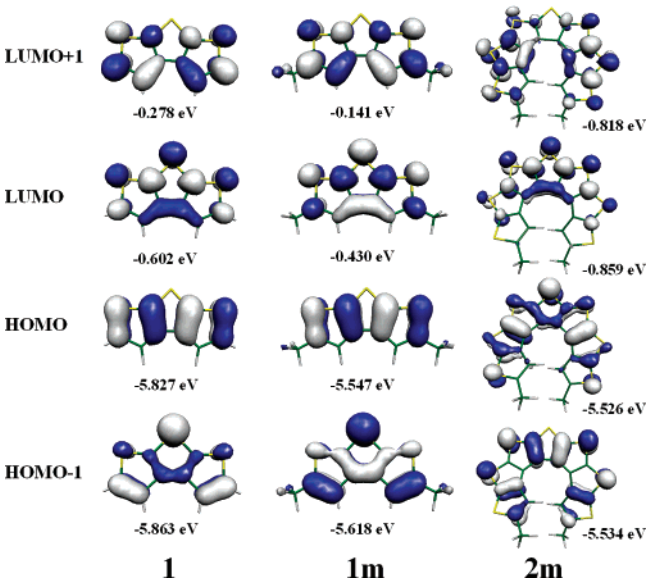

Figure 9. B3LYP/6-31G** electronic density contours (0.03 *e*/bohr^3) and energies for selected MOs of **1**, **1m**, and **2m** around the band gap region.

counterparts in the other half-molecule become stronger. A similar discussion can be made for the Raman stretching vibration of 1409 cm^{-1} regarding the bonding C(4)−C(5) interaction in the HOMO and its symmetry-equivalent C(9)−C(10) counterpart. Therefore, the HOMO−LUMO gap is narrowed to a lower extent along the two Raman modes of 1430 and 1409 cm^{-1}, compared to the stretching vibration giving rise to the strongest Raman feature at 1357 cm^{-1}.

Comparison of the Raman spectra of **1** and **1o** indicates that the most intense Raman lines are upshifted upon replacement of the hydrogens with the alkyl groups at the terminal α-positions.[59] Similar phenomenon has been observed for other two series of α,α′-dimethyl and α,α′-diethyl end-capped oligothiophenes, and it was accounted for in terms of the attainment of a richer π-system for the disubstituted oligothiophene, due to the electronic effect of the *n*-alkyl side chains (positive inductive effect).[60a,b] It should be noted that the Raman spectrum of a sexithiophene end-capped by *n*-thiohexyl groups is almost identical to that of unsubstituted sexithiophene, regardless of the presence of heavy sulfur atoms attached to the outermost α-C_{sp2} atoms in the former oligothiophene.[60c] Therefore, it is not likely that the observed upshift of the Raman spectroscopic profile in **2** may be accounted for by the mass effect on the molecular vibrations or by the lattice dynamics changes between a one-dimensional chain with free or fixed ends.

The B3LYP/6-31G** shapes and energies of the frontier MOs indicate an upshift in energy of both the doubly occupied and empty MOs around the band gap region for the α,α′-dimethyl end-capped **1m** compared to its unsubstituted counterpart **1** (Figure 9). This upshift of approximately 0.15−0.30 eV is slightly more pronounced for the HOMOs, leading to the narrower HOMO−LUMO gap for **1m**, in agreement with the experimental electronic absorption spectra for **1o** and **1**.[27]

Raman spectrum of **2o** shows the strongest peaks at 1392, 1358, 1347, and 1340 cm^{-1}. Correlation of the B3LYP/6-31G** Raman-active vibrational eigenvectors and the electronic density contours related to the frontier MOs of **2m** provides an explanation for these experimental findings. Considering interactions between the C_α and C_β atoms of the three innermost annelated thiophene rings, distortion of **2m** in the direction opposite to the Raman-active mode of 1340 cm^{-1} (Figure 8) leads to weaker antibonding and bonding interactions in the LUMO and HOMO, respectively. Hence, the LUMO is stabilized, while the HOMO is destabilized, along such molecular vibration, as expected for a large vibronic coupling. Similar, though smaller, HOMO−LUMO gap narrowing occurs when the cross-conjugated carbon−carbon framework of **2m** is distorted along the Raman-active ν_{sym}(C═C) stretching vibration of 1347 cm^{-1}, which affects only interactions between the C_α and C_β atoms of the central ring in the LUMO and HOMO. Along the Raman mode of 1358 cm^{-1}, the bonding C(4)−C(5) and C(12)−C(13) interactions in the HOMO of **2m** are strengthened, whereas their symmetry-equivalent C(9)−C(10) and C(15)−C(16) bonding counterparts in the other half of the molecule are softened in a similar way. The same balance occurs between the corresponding antibonding interactions in the LUMO; this is the reason why this ν_{sym}(C═C) Raman mode shows much weaker coupling to the HOMO and LUMO, compared to the 1340-cm^{-1} mode. In addition, the B3LYP/6-

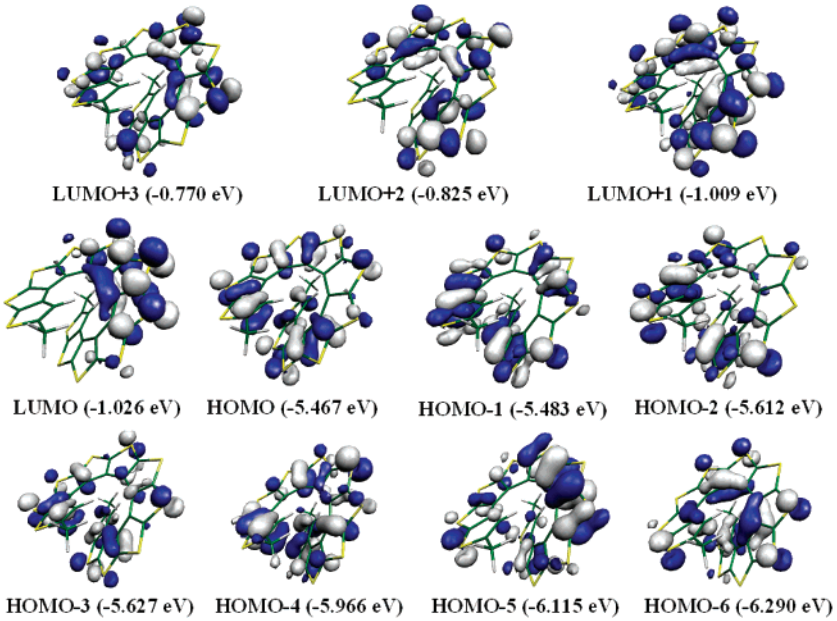

Figure 10. B3LYP/6-31G** electronic density contours (0.03 *e*/bohr^3) and energies for selected MOs of **3m** around the band gap region.

31G** vibrational computations suggest that two nearly degenerate Raman-active modes contribute to the experimental feature at 1392 cm^{-1}.

For **3o**, the strongest Raman scattering at 1323 cm^{-1} is due to a fully in-phase ν_{sym}(C═C) mode located on the five innermost annelated rings, which largely couples to the LUMO. The B3LYP/6-31G** calculations suggest that the experimental Raman feature at 1348 cm^{-1} consists of two overlapping Raman-active modes, both of which are primarily located on outer rings of the oligothiophene. The higher- and lower-energy modes arise from in-phase and out-of-phase ν(C═C) vibrations, respectively. The shapes of the frontier MOs indicate that the higher-energy in-phase mode couples more favorably to both the HOMO and HOMO-1 orbitals than the lower-energy out-of-phase mode. A similar discussion can be made for the Raman line at 1375 cm^{-1}; that is, the B3LYP/6-31G** calculations predict the overlap of another two nearly degenerate Raman-active ν(C═C) modes with opposite phases and located near the terminal thiophene rings of the oligothiophene. As for the modes at 1348 cm^{-1}, the higher-energy in-phase mode couples more favorably to the HOMO and HOMO-1 orbitals than the lower-energy out-of-phase mode. For the Raman scatterings at 1323, 1348, and 1375 cm^{-1}, the strongest modes tend to be located at the thiophene rings closer to the center of the oligothiophene.

Conjugational Properties of Annelated β-Oligothiophenes. Notably, the B3LYP/6-31G** energies of the frontier MOs around the band gap region for annelated β-oligothiophenes **1m**, **2m**, and **3m** show near degeneracies between HOMO and HOMO-1, as well as LUMO and LUMO-1 (Figures 9 and 10). These near-degeneracies are more pronounced for oligomers with a higher number of annelated thiophenes. For **3m**, the six HOMOs may be grouped into three near-degenerate pairs: HOMO/HOMO-1, HOMO-2/HOMO-3, and HOMO-4/HOMO-5; furthermore, the four HOMOs may be viewed as near-degenerate, with the energy difference of 0.16 eV between HOMO and HOMO-3. The increase of near degeneracies, with "clustering" of MOs near the HOMO for the higher oligomers, may be viewed as indicative of electron localization. Such near degeneracies were observed for ladderlike oligomers of biphenylene, in which electron localization is induced by the antiaromatic 4-membered rings; for the biphenylene polymer, the electron localization was indicated by the presence of a narrow energy band near the Fermi level.[61] The electron localization, with narrow energy bands near the Fermi level, is one of the characteristic features of cross-conjugated polymers.[62] Furthermore, the overall patterns of the atomic coefficients of the frontier MOs in **1**, **1m**, and **2m** (Figure 9) are very similar, including significant contributions from the sulfur atoms. In particular, the MOs of **2m** are largely localized on the three center thiophene rings, resembling the MOs of **1** and **1m**, in contrast to the annelated α-oligothiophenes (pentathienoacene and heptathienoacene).[63] This behavior and the finding that enhanced Raman scatterings appear less disperse with the increasing number of the annelated thiophene rings may suggest significant electron localization in these β-oligothiophenes. In other words, the annelated β-oligothiophenes may be viewed as cross-conjugated, in spite of contributions from sulfur atoms to the frontier MOs. These observations and analyses are in agreement with the experimental finding of electron localization in the $(C_2S)_n$ helix with an onset at $n \approx 7$, based upon optical spectroscopy (and electrochemistry) of **1o**−**3o**.[26]

IV. Summary and Conclusions

We have reported the spectroscopic Raman data for α,α'-bis(alkyl) end-capped β-oligothiophenes, with three, seven, and eleven annelated thiophene rings. Analyses based upon B3LYP/6-31G** vibrational calculations indicate that the selective enhancement of a limited number of Raman scatterings, among the many Raman-active molecular vibrations predicted by the optical selection rules, is related to a strong vibronic coupling between selected skeletal ν_{sym}(C═C) stretching modes and the HOMO/LUMO frontier orbitals. The strongest Raman features are assigned to particular skeletal vibrations, with a marked collective character, along which the displacements of the carbon atoms from their equilibrium positions better match the orientations of the bonding/antibonding patterns of the HOMO and LUMO levels, thus leading to a large narrowing of the HOMO−LUMO energy gap. Although this behavior is analogous to that found in typical π-conjugated systems, including α-oligothiophenes, important differences between α-oligothiophenes and the helically annelated β-oligothiophenes were found, pointing to their different conjugational properties. Unlike for α-oligothiophenes, enhanced Raman scatterings of the annelated β-oligothiophenes appear less disperse, with the increasing number of the annelated thiophene rings from three to seven and then to eleven. Furthermore, both atomic coefficients and energies of the frontier molecular orbitals around the band gap are consistent with electron localization in the helically annelated β-oligothiophenes.

Acknowledgment. Research at the University of Málaga was supported by the Ministerio de Educación y Ciencia (MEC) of Spain through Projects BQU2003-03194 and CTQ2006-14987-C02-01, and by the Junta de Andalucía for funding our FQM-0159 scientific group and for Project P06-FQM-01678. R.M.O. is also grateful to MEC for her personal doctoral grant. Research at the University of Nebraska was supported by the National Science Foundation (CHE-0414936). Research at the University of Missouri—Columbia was made possible by Federal Earmark NASA Funds for Bioinformatics Consortium Equipment and additional financial support from Dell, SGI, Sun Microsystems, TimeLogic, and Intel.

Note Added after ASAP Publication. This manuscript was originally published on January 18, 2007. Some of the references have been corrected and WEOs were added to Figure 8. The corrected version was reposted on March 2, 2007.

Supporting Information Available: ^{1}H NMR spectra of **1**, **1o**−**3o**, and 5-octyldithieno[2,3-*b*:3′,2′-*d*]thiophene, Raman spectrum of 5-octyldithieno[2,3-*b*:3′,2′-*d*]thiophene, animations of computed Raman spectra of **1m**−**3m**, and computational details. This material is available free of charge via the Internet at http://pubs.acs.org.

References and Notes

(1) Barbarella, G.; Melucci, M.; Sotgiu, G. *Adv. Mater.* **2005**, *17*, 1581.
(2) Katz, H. E.; Bao, Z.; Gilat, S. L. *Acc. Chem. Res.* **2001**, *34*, 359.
(3) Fichou, D. *J. Mater. Chem.* **2000**, *10*, 571.
(4) Roncali, J. *Acc. Chem. Res.* **2000**, *33*, 147.
(5) Tour, J. M. *Acc. Chem. Res.* **2000**, *33*, 791.
(6) Izumi, T.; Kobayashi, S.; Takimiya, K.; Aso, Y.; Otsubo. T. *J. Am. Chem. Soc.* **2003**, *125*, 5286.
(7) (a) Krömer, J.; Rios-Carreras, I.; Fuhrmann, G.; Musch, C.; Wunderlin, M.; Debaerdemaeker, T.; Mena-Osteritz, E.; Bäuerle, P. *Angew. Chem., Int. Ed.* **2000**, *39*, 3481. (b) Gesquiere, A.; Jonkheijm, P.; Schenning, A. P. H. J.; Mena-Osteritz, E.; Bäuerle, P.; de Feyter, S.; de Schryver, F. C.; Meijer, E. W. *J. Mater. Chem.* **2003**, *13*, 2164. (c) Caras-Quintero, D.; Bäuerle, P. *Chem. Commun.* **2004**, 926.
(8) Casado, J.; Pappenfus, T. M.; Miller, L. L.; Mann, K. R.; Orti, E.; Viruela, P. M.; Pou-Amerigo, R.; Hernandez, V.; Lopez Navarrete, J. T. *J. Am. Chem. Soc.* **2003**, *125*, 2524.
(9) Huynh, W. U.; Dittmer, J. J.; Alivastatos, A. P. *Science* **2002**, *295*, 2425.

(10) Horowitz, G.; Bachet, B.; Yassar, A.; Lang, P.; Demanze, F.; Fave, J.-L.; Garnier, F. *Chem. Mater.* **1995**, *7*, 1337.

(11) (a) Murphy, A. R.; Fréchet, J. M. J.; Chang, P.; Lee, J.; Subramanian, V. *J. Am. Chem. Soc.* **2004**, *126*, 1596.(b) Liu, J.; Kadnikova, E. N.; Liu, Y.; McGehee, M. D.; Fréchet, J. M. *J. Am. Chem. Soc.* **2004**, *126*, 9486.

(12) Mazaki, Y.; Kobayashi, K. *Tetrahedron Lett.* **1989**, *30*, 3315.

(13) Sato, V.; Mazaki, Y.; Kobayashi, K.; Kobayashi, T. *J. Chem. Soc., Perkin Trans. 2* **1992**, 765.

(14) Zhang, X.; Matzger, A. J. *J. Org. Chem.* **2003**, *68*, 9813.

(15) Zhang, X.; Côté, A. P.; Matzger, A. J. *J. Am. Chem. Soc.* **2005**, *127*, 10502.

(16) Mazzeo, M.; Vitale, V.; Della Sala, F.; Anni, M.; Barbarella, G.; Favaretto, L.; Sotgiu, G.; Cingolani, R.; Gigli, G. *Adv. Mater.* **2005**, *17*, 34.

(17) Xiao, K.; Liu, Y.; Qi, T.; Zhang, W.; Wang, F.; Gao, J.; Qiu, W.; Ma, Y.; Cui, G.; Chen, S.; Zhan, X.; Yu, G.; Qin, J.; Hu, W.; Zhu, D. *J. Am. Chem. Soc.* **2005**, *127*, 13281.

(18) Ye, X.-S.; Wong, H. N. C. *J. Org. Chem.* **1997**, *62*, 1940.

(19) Hart, H.; Sasaoka, M. *J. Am. Chem. Soc.* **1978**, *100*, 4326.

(20) (a) Kauffman, T.; Greving, B.; Köning, J.; Mitschker, A.; Woltermann, A. *Angew. Chem., Int. Ed. Engl.* **1975**, *14*, 713. (b) Kauffman, T. *Angew. Chem., Int. Ed. Engl.* **1979**, *18*, 1.

(21) de Jong, F.; Janssen, M. J. *J. Org. Chem.* **1971**, *36*, 1998.

(22) Nenajdenko, V. G.; Sumerin, V. V.; Chernichenko, K. Y.; Balenkova, E. S. *Org. Lett.* **2004**, *6*, 3437.

(23) Rajca, A.; Wang, H.; Pink, M.; Rajca, S. *Angew. Chem., Int. Ed.* **2000**, *39*, 4481.

(24) Miyasaka, M.; Rajca, A. *Synlett.* **2004**, 177.

(25) Rajca, A.; Miyasaka, M.; Pink, M.; Wang, H. Rajca, S. *J. Am. Chem. Soc.* **2004**, *126*, 15211.

(26) Miyasaka, M.; Rajca, A.; Pink, M.; Rajca, S. *J. Am. Chem. Soc.* **2005**, *127*, 13806.

(27) Miyasaka, M.; Rajca, A. *J. Org. Chem.* **2006**, *71*, 3264.

(28) Xue, J.; Forrest, S. R. *Appl. Phys. Lett.* **2001**, *79*, 3714.

(29) Tanaka, H.; Okano, Y.; Kobayashi, H.; Suzuki, W.; Kobayashi, A. *Science* **2001**, *291*, 285.

(30) Williams, J. M.; Schultz, A. J.; Geiser, U.; Carlson, K. D.; Kini, A. M.; Wang, H. H.; Kwok, W.-K.; Whangbo, M.-H.; Schirber, J. E. *Science* **1991**, *252*, 1501.

(31) Nielsen, M. B.; Diederich, F. *Chem. Rev.* **2005**, *105*, 1837.

(32) Nielsen, M. B.; Schreiber, M.; Baek, Y. G.; Seiler, P.; Lecomte, S.; Boudon, C.; Tykwinski, R. R.; Gisselbrecht, J.-P.; Gramlich, V.; Skinner, P. J.; Bosshard, C.; Günther, P.; Gross, M.; Diederich, F. *Chem.*−*Eur. J.* **2001**, *7*, 3263.

(33) (a) Zhao, Y.; Tykwinski, R. R. *J. Am. Chem. Soc.* **1999**, *121*, 458. (b) Zhao, Y.; McDonald, R.; Tykwinski, R. R. *J. Org. Chem.* **2002**, *67*, 2805.

(34) Gaab, K. M.; Thompson, A. L.; Xu, J.; Martinez, T. J.; Bardeen, C. J. *J. Am. Chem. Soc.* **2003**, *125*, 9288.

(35) Londergan, T. M.; You, Y.; Thompson, M. E.; Weber, W. P. *Macromolecules* **1998**, *31*, 2784.

(36) Wilson, J. N.; Windscheif, P. M.; Evans, U.; Myrick, M. L.; Bunz, U. H. F. *Macromolecules* **2002**, *35*, 8681.

(37) Klokkenburg, M.; Lutz, M.; Spek, A. L.; van der Maas, J. H.; van Walree, C. A. *Chem.*−*Eur. J.* **2003**, *9*, 3544.

(38) (a) Zerbi, G.; Castiglioni, C.; Del Zoppo, M. *Electronic Materials: The Oligomer Approach*; Wiley−VCH: Weinheim, 1998; p 345. (b) Castiglioni, C.; Gussoni, M.; Lopez Navarrete, J. T.; Zerbi, G. *Solid State Commun.* **1988**, *65*, 625. (c) Lopez Navarrete, J. T.; Zerbi, G. *J. Chem. Phys.* **1991**, *94*, 957 and 965. (d) Hernandez, V.; Castiglioni, C.; Del Zoppo, M.; Zerbi, G. *Phys. Rev. B* **1994**, *50*, 9815. (e) Agosti, E.; Rivola, M.; Hernandez, V.; Del Zoppo, M.; Zerbi, G. *Synth. Met.* **1999**, *100*, 101. (f) Zerbi, G. *Handbook of Conducting Polymers*; Marcel Dekker: New York, 1998.

(39) (a) Ruiz Delgado, M. C.; Casado, J.; Hernandez, V.; Lopez Navarrete, J. T.; Fuhrmann, G.; Bauerle, P. *J. Phys. Chem. B* **2004**, *108*, 3158. (b) Casado, J.; Hernandez, V.; Ponce Ortiz, R.; Ruiz Delgado, M. C.; Lopez Navarrete, J. T.; Fuhrmann, G.; Bauerle, P. *J. Raman Spectrosc.* **2004**, *35*, 592.

(40) VCD study of carbon−sulfur (7)helicene (Figure 1): Friedman, T. B.; Cao, X.; Rajca, A.; Wang, H.; Nafie, L. A. *J. Phys. Chem. A* **2003**, *107*, 7692.

(41) First principle calculation of Raman spectrum for (6)helicene in the ν(C−H) region: Dobrowolski, J. C. *J. Mol. Struct.* **2003**, *651*−*653*, 607.

(42) (a) Katz, T. J. *Angew. Chem., Int. Ed.* **2000**, *39*, 1921. (b) Han, S.; Anderson, D. R.; Bond, A. D.; Chu, H. V.; Disch, R. L.; Holmes, D.; Schulman, J. M.; Teat, S. J.; Vollhardt, K. P. C.; Whitener, G. D. *Angew. Chem., Int. Ed.* **2002**, *41*, 3227. (c) Xu, Y.; Zhang, Y. X.; Sugiyama, H.; Umano, T.; Osuga, H.; Tanaka, K. *J. Am. Chem. Soc.* **2004**, *126*, 6566. (d) K. Shiraishi, K.; Rajca, A.; Pink, M.; Rajca, S. *J. Am. Chem. Soc.* **2005**, *127*, 9312. (e) Collins, S. K.; Vachon, M. P. *Org. Biomol. Chem.* **2006**, *4*, 2518.

(43) (a) Verbiest, T.; Van Elshocht, S.; Kauranen, M.; Hellemans, L.; Snauwaert, J.; Nuckolls, C.; Katz, T. J.; Persoons, A. *Science* **1998**, *282*, 913. (b) Field, J. E.; Muller, G.; Riehl, J. P.; Venkataraman, D. *J. Am. Chem. Soc.* **2003**, *125*, 11808. (c) Miyasaka, M.; Rajca, A.; Pink, M.; Rajca, S. *Chem.*−*Eur. J.* **2004**, *10*, 6531.

(44) Raman, spectra of radialenes: Iyoda, M.; Tanaka, S.; Otani, H.; Nose, M.; Oda, M. *J. Am. Chem. Soc.* **1988**, *110*, 8494.

(45) Cravino, A.; Neugebauer, H.; Luzzati, S.; Catellani, M.; Petr, A.; Dunsch, L.; Sariciftci, N. S. *J. Phys. Chem. B* **2002**, *106*, 3583.

(46) Frisch, M. J.; Trucks, G. W.; Schlegel, H. B.; Scuseria, G. E.; Robb, M. A.; Cheeseman, J. R.; Montgomery, J. A. Jr.; Vreven, T.; Kudin, K. N.; Burant, J. C.; Millam, J. M.; Iyengar, S. S.; Tomasi, J.; Barone, V.; Mennucci, B.; Cossi, M.; Scalmani, G.; Rega, N.; Petersson, G. A.; Nakatsuji, H.; Hada, M.; Ehara, M.; Toyota, K.; Fukuda, R.; Hasegawa, J.; Ishida, M.; Nakajima, T.; Honda, Y.; Kitao, O.; Nakai, H.; Klene, M.; Li, X.; Knox, J. E.; Hratchian, H. P.; Cross, J. B.; Adamo, C.; Jaramillo, J.; Gomperts, R.; Stratmann, R. E.; Yazyev, O.; Austin, A. J.; Cammi, R.; Pomelli, C.; Ochterski, J. W.; Ayala, P. Y.; Morokuma, K.; Voth, G. A.; Salvador, P.; Dannenberg, J. J.; Zakrzewski, V. G.; Dapprich, S.; Daniels, A. D.; Strain, M. C.; Farkas, O.; Malick, D. K.; Rabuck, A. D.; Raghavachari, K.; Foresman, J. B.; Ortiz, J. V.; Cui, Q.; Baboul, A. G.; Clifford, S.; Cioslowski, J.; Stefanov, B. B.; Liu, G.; Liashenko, A.; Piskorz, P.; Komaromi, I.; Martin, R. L.; Fox, D. J.; Keith, T.; Al-Laham, M. A.; Peng, C. Y.; Nanayakkara, A.; Challacombe, M.; Gill, P. M. W.; Johnson, B.; Chen, W.; Wong, M. W.; Gonzalez, C.; Pople, J. A. *Gaussian 03*, revision B.04; Gaussian Inc.: Pittsburgh PA, 2003.

(47) Becke, A. D. *J. Chem. Phys.* **1993**, *98*, 1372.

(48) Stephens, P. J.; Devlin, F. J.; Chabalowski, F. C. F.; Frisch, M. J. *J. Phys. Chem.* **1994**, *98*, 11623.

(49) Novoa, J. J.; Sosa, C. *J. Phys. Chem.* **1995**, *99*, 15837.

(50) Scott, A. P.; Radom, L. *J. Phys. Chem.* **1996**, *100*, 16502.

(51) Rauhut, G.; Pulay, P. *J. Phys. Chem.* **1995**, *99*, 3093.

(52) Francl, M. M.; Pietro, W. J.; Hehre, W. J.; Binkley, J. S.; Gordon, M. S.; Defrees, D. J.; Pople, J. A. *J. Chem. Phys.* **1982**, *77*, 3654.

(53) Portmann, S.; Lüthi, H. P. *Chimia* **2000**, *54*, 766−770.

(54) (a) Ehrendorfer, Ch.; Karpfen, A. *J. Phys. Chem.* **1994**, *98*, 7492. (b) Ehrendorfer, Ch.; Karpfen, A. *J. Phys. Chem.* **1995**, *99*, 5341. (c) Brocks, G. *Phys. Rev. B* **1997**, *55*, 6816.

(55) Sakamoto, A.; Furukawa, Y.; Tasumi, M. *J. Phys. Chem.* **1994**, *98*, 4635.

(56) (a) Yokonuma, N.; Furukawa, Y.; Tasumi, M.; Kuroda, M.; Nakayama, J. *Chem. Phys. Lett.* **1996**, *255*, 431. (b) Harada, I.; Furukawa, Y. *Vibrational Spectra and Structure*; Durig, J., Ed.; Elsevier: Amsterdam 1991; Vol. 19, p 369.

(57) (a) Hernandez, V.; Casado, J.; Ramirez, F. J.; Zotti, G.; Hotta, S.; Lopez Navarrete, J. T. *J. Chem. Phys.* **1996**, *104*, 9271. (b) Moreno Castro, C.; Ruiz Delgado, M. C.; Hernandez, V.; Hotta, S.; Casado, J.; Lopez Navarrete, J. T. *J. Chem. Phys.* **2002**, *116*, 10419. (c) Moreno Castro, C.; Ruiz Delgado, M. C.; Hernandez, V.; Shirota, Y.; Casado, J.; Lopez Navarrete, J. T. *J. Phys. Chem. B* **2002**, *106*, 7163. (d) Ruiz Delgado, M. C.; Hernandez, V.; Lopez Navarrete, J. T.; Tanaka, S.; Yamashita, Y. *J. Phys. Chem. B* **2004**, *108*, 2516. (e) Casado, J.; Ponce Ortiz, R.; Ruiz Delgado, M. C.; Azumi, R.; Oakley, R. T.; Hernandez, V.; Lopez Navarrete, J. T. *J. Phys. Chem. B* **2005**, *109*, 10115.

(58) (a) Casado, J.; Hernandez, V.; Hotta, S.; Lopez Navarrete, J. T. *J. Chem. Phys.* **1998**, *109*, 10419. (b) Casado, J.; Hernandez, V.; Hotta, S.; Lopez Navarrete, J. T. *Adv. Mater.* **1998**, *10*, 1458. (c) Casado, J.; Miller, L. L.; Mann, K. R.; Pappenfus, T. M.; Kanemitsu, Y.; Orti, E.; Viruela, P. M.; Pou-Amerigo, P.; Hernandez, V.; Lopez Navarrete, J. T. *J. Phys. Chem. B* **2002**, *106*, 3872. (d) Casado, J.; Miller, L. L.; Mann, K. R.; Pappenfus, T. M.; Hernandez, V.; Lopez Navarrete, J. T. *J. Phys. Chem. B* **2002**, *106*, 3597. (e) Casado, J.; Ruiz Delgado, M. C.; Shirota, Y.; Hernandez, V.; Lopez Navarrete, J. T. *J. Phys. Chem. B* **2003**, *107*, 2637.

(59) The replacement of hydrogen with the octyl group at one of the terminal α positions gives rise to an intermediate upshift of the most intense Raman lines in the 1400-cm^{-1} region, as shown by Raman spectrum of 5-octyldithieno(2,3-*b*:3′,2′-*d*)thiophene (Figure S6, Supporting Information).

(60) (a) Casado, J.; Ramirez, F. J.; Hotta, S.; Lopez Navarrete, J. T.; Hernandez, V. *Synth. Met.* **1997**, *84*, 571. (b) Casado, J.; Hotta, S.; Hernandez, V.; Lopez Navarrete, J. T. *J. Phys Chem. A* **1999**, *103*, 816. (c) Casado, J.; Katz, H. E.; Hernandez, V.; Lopez Navarrete, J. T. *J. Phys Chem. B* **2002**, *106*, 2488.

(61) Rajca, A.; Safronov, A.; Rajca, S.; Ross, C. R., II; Stezowski, J. J. *J. Am. Chem. Soc.* **1996**, *118*, 7272.

(62) (a) Nath, K.; Taylor, P. L. *Mol. Cryst. Liq. Cryst.* **1990**, *180B*, 389. (b) Dietz, F.; Tyutyulkov, N. *Res. Adv. Macromolecules* **2000**, *1*, 73.

(63) Malave Osuna, R.; Zhang, X.; Matzger, A. J.; Hernandez, V.; Lopez Navarrete, J. T. *J. Phys Chem. A* **2006**, *110*, 5058.